Taylor & Francis
Taylor & Francis Group

Philosophical Magazine

ISSN: 1478-6435 (Print) 1478-6443 (Online) Journal homepage: http://www.tandfonline.com/loi/tphm20

Improving the ballistic AC conductivity through quantum resonance in branched nanowires

Vicenta Sánchez & Chumin Wang

To cite this article: Vicenta Sánchez & Chumin Wang (2015) Improving the ballistic AC conductivity through quantum resonance in branched nanowires, Philosophical Magazine, 95:3, 326-333, DOI: 10.1080/14786435.2014.1000995

To link to this article: http://dx.doi.org/10.1080/14786435.2014.1000995

Philosophical Magazine, 2015
Vol. 95, No. 3, 326–333, http://dx.doi.org/10.1080/14786435.2014.1000995

Improving the ballistic AC conductivity through quantum resonance in branched nanowires

Vicenta Sánchez[a] and Chumin Wang[b]*

[a]*Facultad de Ciencias, Departamento de Física, Universidad Nacional Autónoma de México, Apartado Postal 70-542, 04510, D.F., México, Mexico;* [b]*Instituto de Investigaciones en Materiales, Universidad Nacional Autónoma de México, Apartado Postal 70-360, 04510, D.F. México, Mexico*

(*Received 25 March 2014; accepted 17 December 2014*)

Frequency-dependent electrical conductivity is studied by means of the Kubo-Greenwood formula and a real-space renormalization plus convolution method. An analytical solution of the alternating current (AC) conductivity is found for periodic chains. In this article, we report enhancements to this ballistic AC conductivity when periodically or quasiperiodically placed Fano-Anderson impurities are introduced to an otherwise periodic chain, which is connected to two semi-infinite periodic leads at its ends. Moreover, the temperature effects on these resonant AC conducting states are remarkably different in periodic and in quasiperiodic systems. Finally, such enhancement is further analysed in branched nanowires with a small cross section.

Keywords: electronic transport; Kubo-Greenwood formula; AC conductivity; branched nanowires

1. Introduction

The wave behaviour of quantum particles is exhibited in crystalline solids by the formation of diffraction patterns, which are also observed in quasicrystals despite their lack of translational symmetry [1]. The electronic transport in solids with a large number of impurities is still an unclear issue, where the interference between the electronic wavefunction and aperiodic potentials has multiple consequences. Recently, branched nanowires with tunable three-dimensional (3D) morphology have been obtained, and they have wide applications in energy conversion and storage devices [2]. Nonlinear electrical properties of branched nanowires have also been reported [3]. In this article, we report an impurity-induced enhancement of the alternating current (AC) conductivity, which could be even larger than the ballistic one present in periodic systems.

The electronic behaviour in crystalline solids is traditionally studied using the reciprocal lattice method [4], and it becomes inadequate or useless when the system loses the translational symmetry. In consequence, most of the studies of non-periodic systems have been carried out in finite clusters with or without the periodic boundary condition. The former frequently introduces undesirable contributions derived from the artificial periodic boundary condition and the latter overemphasizes the molecular character of

*Corresponding author. Email: chumin@unam.mx

discrete energy spectra. In this work, we use a fully real-space renormalization plus convolution method to study the electronic transport in a non-periodic macroscopic system under an oscillating electric field. This method has the advantage of being numerically accurate and computationally efficient, that is able to address 10^{24} non-periodically located atoms without introducing additional approximations during the calculation through Kubo-Greenwood formula [5].

2. Fano-Anderson impurities

In this section, the electronic transport in periodic chains with periodic and quasiperiodically placed Fano-Anderson impurities [6] will be addressed. In order to isolate the impurity effects on the electronic transport, let us consider a single-band tight-binding Hamiltonian with null self-energies and a constant hopping integral t given by

$$H = t \sum_{\langle i,j \rangle} \{|i\rangle\langle j| + |j\rangle\langle i|\} + t \sum_{j \in \Theta} \{|j\rangle\langle s| + |s\rangle\langle j|\}, \tag{1}$$

where nearest neighbour atoms i and j, indicated by $\langle i, j \rangle$, belong to the main system which could be a periodic chain or a periodic nanowire, s denotes the Fano-Anderson impurity atoms (violet balls in Figure 1) with null self-energy and Θ is a subset of the main system where the impurity atoms are connected. Despite that the system has a unique hopping integral t, the Fano-Anderson impurities modify the local coordination number of several atoms. For example, the coordination number is two for the unperturbed sites and three at impurity-connected sites for one-dimensional (1D) systems, as shown in Figure 1(a).

To model the AC conductivity within the linear response theory, we use the Kubo-Greenwood formula given by Kramer and MacKinnon [7]

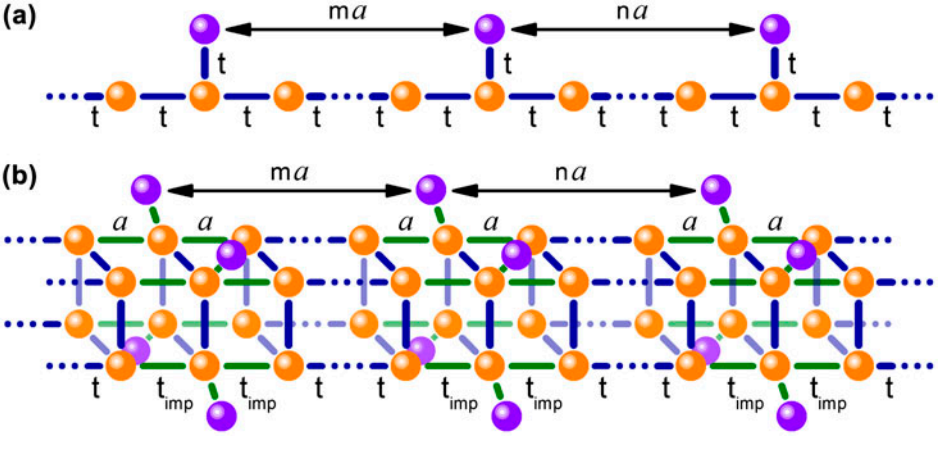

Figure 1. (colour online) Schematic representation of (a) a periodic atomic chain and (b) a multi-channel branched nanowire. Both systems, formed by null self-energy atoms (orange balls) and bonds described by hopping integrals t (blue lines), possess periodically or quasiperiodically placed Fano-Anderson impurities (violet balls) with three perturbed hopping integrals t_{imp} (green lines) around each impurity.

$$\sigma(\mu,\omega,T)=\frac{2e^2\hbar}{\Omega\,\pi\,m^2}\int_{-\infty}^{\infty}dE\frac{f(E)-f(E+\hbar\,\omega)}{\hbar\,\omega}Tr[p\mathrm{Im}G^{+}(E+\hbar\,\omega)p\,\mathrm{Im}G^{+}(E)],\quad(2)$$

where $p=(i\,m/\hbar)[H,x]=t\sum_j\{|j\rangle\langle j+1|-|j\rangle\langle j-1|\}$ is the projection of the momentum operator along the applied electrical field, Ω is the system volume, $G^{+}(E)=G(E+i\,\eta)$ is the retarded one-particle Green's function and $f(E)=\{1+\exp[(E-\mu)/k_BT]\}^{-1}$ is the Fermi–Dirac distribution with the chemical potential μ and temperature T.

For a periodic chain of N atoms connected to two semi-infinite periodic leads with the same t, the AC conductivity at $T=0$ K has an analytical solution of Sanchez and Wang [5]

$$\sigma(\mu,\omega,0)=\frac{8\,e^2t^2a}{\pi\,(N\ -1)\,\hbar^3\omega^2}\left[1-\left(\frac{\mu}{2t}\right)^2\right]\left\{1-\cos\left[\frac{(N\ -1)\,\hbar\,\omega}{2t\sqrt{1-(\mu/2t)^2}}\right]\right\}\Xi(2|t|-|\mu|),\quad(3)$$

where $\Xi(x)$ is the Heaviside step function. The direct current (DC) conductivity with $\omega=0$ is as follows [8]:

$$\sigma_P\equiv\sigma(\mu,0,0)=\frac{e^2a}{\pi\hbar}(N-1).\quad(4)$$

Along this periodic chain, multiple single-atom Fano-Anderson impurities with null self-energy can be connected to the chain through a hopping integral t, as schematically shown in Figure 1(a). These impurities may be placed periodically when $m=n$ or quasiperiodically when the impurity separations ma and na are ordered following the Fibonacci sequence of generation k defined by $F(k)=F(k-1)+F(k-2)$ with initial conditions of $F(1)=na$ and $F(2)=ma$, for example, $F(5)=(ma)(na)(ma)(ma)(na)$. Numerical calculations of the AC conductivity in both systems were carried out using a previously developed renormalization method [5], in which renormalized self-energies of t^2/E are added to those atoms connected to the Fano-Anderson impurities [9]. For the periodic case, we take $m=n=256$, which leads to 524,288 symmetrically placed impurities in a chain of $2^{27}=134,217,728$ atoms and the impurity location subset is $\Theta=\{128,\ 384,\ 640,\ \cdots,\ 134,217,600\}$. For the quasiperiodic case, the impurities are introduced every $m=233$ or $n=144$ atoms following the Fibonacci sequence, yielding to 514,230 impurities in a Fibonacci chain with $k=40$ of 165,580,142 atoms, that is $\Theta=\{90,\ 323,\ 467,\ 700,\ \cdots,\ 165,579,998\}$. Both chains are connected to two semi-infinite periodic leads with null self-energies and hopping integral t.

In Figure 2, the AC conductivities (σ) at zero (blue solid circles) and finite (red open circles) temperatures are plotted vs. the applied electric field oscillating frequency (ω) for the mentioned linear chains with (a) periodically and (b) quasiperiodically placed Fano-Anderson impurities, in comparison with the AC conductivity of Equation (3) for a pure periodic chain (green lines). In their insets, (a′ and b′) the DC conductivity spectra and (a″, a‴, b″ and b‴) their magnifications are shown, where the chemical potentials $\mu_0=0.0237999975917|t|$ for the periodic and $\mu_0=0.381036836269|t|$ for the quasiperiodic cases are indicated by orange lines. An imaginary part of energy of $\eta=10^{-15}|t|$ and an interval of $[\mu_0-\hbar\omega-2k_BT,\ \mu_0+2k_BT]$ for numerical integrations

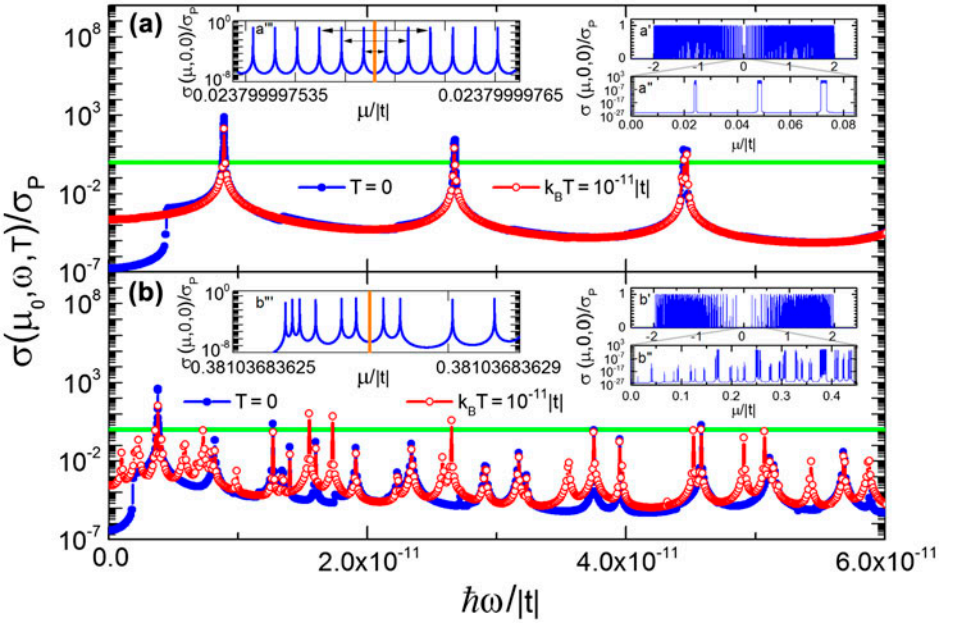

Figure 2. (colour online) Electric conductivity (σ) as a function of applied electric field oscillating frequency (ω) for a periodic chain with (a) periodically and (b) quasiperiodically placed single-atom Fano-Anderson impurities for zero (blue solid circles) and finite (red open circles) temperatures, in comparison with the ballistic AC conductivity (green solid lines). Inset: DC conductivity spectra and their magnifications of a periodic chain with (a′, a″ and a‴) periodically and (b′, b″ and b‴) quasiperiodically placed impurities, where chemical potential μ_0 is indicated by orange solid lines and transitions between first-, third- and fifth-neighbouring peaks are marked by arrows.

were taken, since no significant changes were found beyond these values, as discussed in Ref. [5] for η. Observe the resonant peaks in Figure 2(a), whose maximum reaches to a value of $737\sigma_P$ and its frequency can be predicted by calculating the energy difference of DC-conductivity peaks, as indicated by the arrows in inset (a‴).

For finite temperatures, the AC conductivity spectrum of Figure 2(a) only softens, in contrast to the appearance of new resonant peaks in Figure 2(b). To search the origin of this difference, the trace $Tr[p\mathrm{Im}G^+(E+\hbar\omega)p\mathrm{Im}G^+(E)]$ is plotted using the colour scale in Figures 3(a) for periodic and 3(b) for quasiperiodic cases. First, observe the DC conductivity spectra at $\omega = 0$ and each maximum in these spectra bifurcates when $\omega > 0$ because the trace has two poles: one from $G^+(E)$ and the other from $G^+(E+\hbar\omega)$. Furthermore, for $\omega > 0$, the trace gets maximums only by crossing two peaks that in DC conductivity spectra are first neighbours, third neighbours and so on, due to their wavefunction parity. Now, at zero temperature, one gets an AC conductivity resonant peak when a maximum of the trace is found in the integration interval of $[\mu_0 - \hbar\omega, \mu_0]$. For finite temperatures, this integration interval becomes larger, capturing maximums at new frequencies for quasiperiodic case, in contrast to the periodic impurity case.

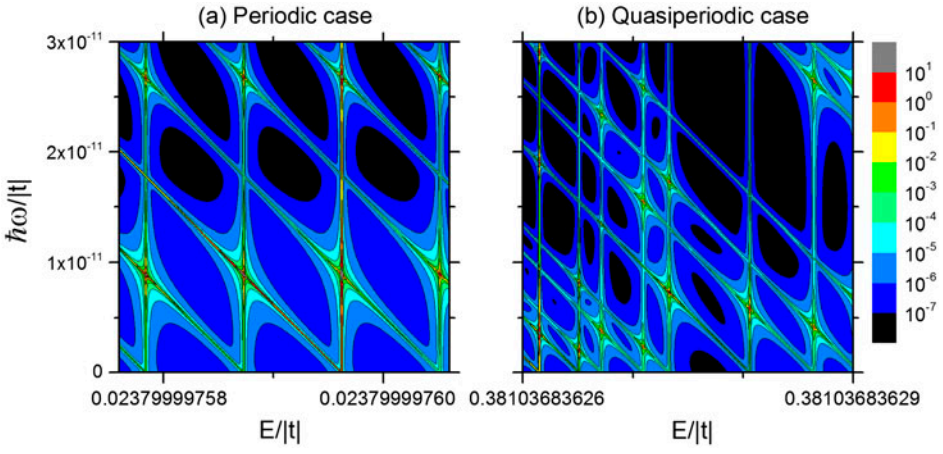

Figure 3. (colour online) Trace $\{Tr[p\mathrm{Im}G^{+}(E+\hbar\,\omega)p\mathrm{Im}G^{+}(E)]\}$ in colour scale plotted as a function of the energy (E) and frequency (ω) for a periodic chain with (a) periodically and (b) quasiperiodically placed single-atom Fano-Anderson impurities.

3. Branched nanowires

The real-space renormalization method can be combined with the convolution theorem to study multidimensional systems when the Hamiltonian is separable, that is $H = H_{\|} \otimes I_{\perp} + I_{\|} \otimes H_{\perp}$, being $H_{\|}$ ($I_{\|}$) and $H_{\perp}$ ($I_{\perp}$), respectively, the Hamiltonian (the identity matrix) of the parallel and perpendicular subsystem with respect to the applied electric field. Actually, the tight-binding Hamiltonian (1) is separable, and then, the electrical conductivity can be expressed as [5]

$$\sigma(\mu,\omega,T) = \frac{1}{\Omega_{\perp}} \sum_{\beta} \sigma^{\|}(\mu - E_{\beta},\omega,T), \tag{5}$$

where $\sigma^{\|}$ is the electrical conductivity of the parallel subsystem; $\Omega_{\perp}$ and E_{β} are, respectively, the volume and the eigenenergies of the perpendicular subsystem, that is $H_{\perp}|\beta\rangle = E_{\beta}|\beta\rangle$.

In particular, this renormalization plus convolution method can be used for studying the electronic transport in kinked or zigzag nanowires [10] and nanowire heterostructures [11], as well as branched nanowires [12]. Let us consider two four-channel branched nanowires, first with periodically and second with quasiperiodically placed single-atom Fano-Anderson impurities, as schematically shown in Figure 1(b), where three perturbed hopping integrals (t_{imp}) due to lattice relaxation are introduced around each impurity. The perpendicular subsystem of these nanowires consists of four atoms with zero self-energy interconnected between nearest neighbours by the same hopping integral t, which leads to eigenenergies of $E_{\beta} = -2t,\ 0,\ 0,\ 2t$. The impurity location and lengths of these nanowires are the same as the single chains discussed in the last section. The ends of these nanowires are connected to two semi-infinite periodic nanowires with the same cross section.

The zero-temperature AC conductance is defined as $g(\mu,\omega,0) \equiv \sigma(\mu,\omega,0)\Omega_{\perp}/\Omega_{\parallel}$, where $\Omega_{\parallel}$ is the system length and $g_0 \equiv 2e^2/h$ is the electrical conductance quantum. In Figure 4, $g(\mu,\omega,0)$ of branched nanowires with (a) periodically and (b) quasiperiodically placed impurities is plotted vs. t_{imp} for fixed electronic densities of (a) $\rho = 0.45233569415$ and (b) $\rho = 0.45273411969$, where $\rho = \frac{1}{N}\int_{-\infty}^{\mu} DOS(E)dE$ is the electronic density per atom, $DOS(E) = -\mathrm{Im}\{Tr[G^{+}(E)]\}/\pi$ is the density of states (DOS), and N is the total number of atoms in the system. In fact, in order to maintain the total number of electrons in the system, μ should vary (a) from $-0.171594623933365|t|$ to $-0.171594623900110|t|$ and (b) from $-0.174869809624280|t|$ to $-0.174869047139636|t|$, when t_{imp} increases from $0.7t$ to $1.3t$. Imaginary parts of energy of $\eta = 10^{-15}|t|$ and $\eta = 10^{-5}|t|$ were taken for the numerical calculations of $g(\mu,\omega,0)$ and $DOS(E)$, respectively. Observe in Figure 4 the truly large values of resonant $g(\mu,\omega,0)$ and their small variation of (a) 0.05% for the periodic case and (b) 3.7% for the quasiperiodic case, when t_{imp} has a variation of ±30%. Note also that the larger variation of $g(\mu,\omega,0)$ in Figure 4(b) could be related to its $\Delta\mu \approx 7.6 \times 10^{-7}|t|$, instead of $\Delta\mu \approx 3.3 \times 10^{-11}|t|$ for the periodic case, since DOS of the quasiperiodic case is more sensitive to the lattice relaxation around Fano-Anderson impurities. It is important to mention that for all analysed electronic densities, we

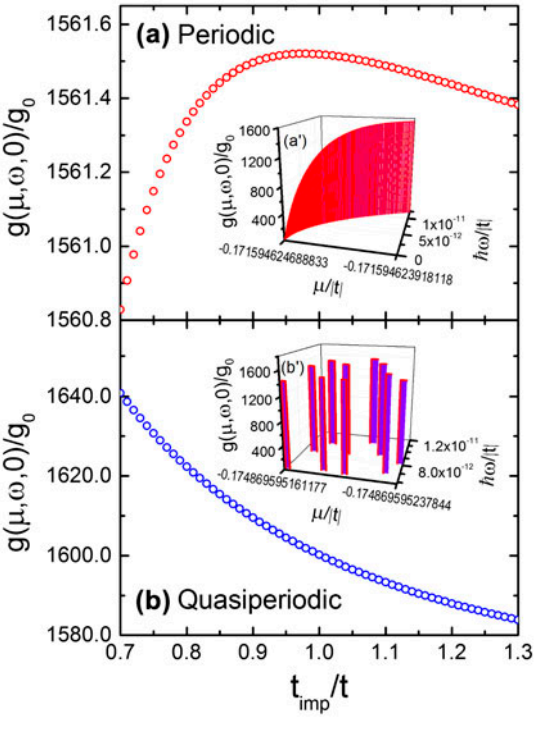

Figure 4. (colour online) Zero-temperature AC electrical conductance [g(μ,ω,0)] vs. the perturbed hopping integral (t_{imp}) for fixed electronic densities of (a) $\rho = 0.45233569415$ and (b) $\rho = 0.45273411969$ in branched four-channel nanowires with (a) periodically and (b) quasiperiodically placed single-atom Fano-Anderson impurities. Insets: g(μ,ω,0) as functions of frequency (ω) and chemical potential (μ).

observe a small variation of $g(\mu,\omega,0)$, but its behaviour as a function of $t_{\rm imp}$ could be different.

The AC conductance spectra $g(\mu,\omega,0)$ of the same branched nanowires of Figure 4(a) and (b) with $t_{\rm imp} = t$ as a function of μ and ω are shown in insets 4(a′) for the periodic case and in 4(b′) for the quasiperiodic case. As in 1D systems, there are many resonant conducting states, whose AC conductance can be much larger than the ballistic one. For nanowires with periodically placed Fano-Anderson impurities, we observe in Figure 4(a) an almost uniformly increase of the resonant frequency associated with a gradual augment of the width in μ space, in contrast to a non-uniform distribution of resonant modes in the frequency space for branched nanowires with quasiperiodically placed impurities, as shown in Figure 4(b).

In Figure 5, the temperature dependence of $g(\mu,\omega,T)$ is plotted for the same branched nanowire of Figure 4(a) and four values of μ, whose locations in the DOS and in the zero-temperature DC conductance $[g(\mu,0,0)]$ spectra are shown in the insets. The resonant frequencies for each μ are specified in the figure. An imaginary part of energy of $\eta = 10^{-15}|t|$ and intervals of $[\mu_j - \hbar\omega_j - 2k_BT,\ \mu_j + 2k_BT]$ for numerical integrations with $j = 1,\ 2,\ 3,$ and 4 were taken. Observe the general decay behaviour of $g(\mu_j,\omega_j,T)$ with the temperature, where their room temperature values are at least two orders of magnitude larger than the zero-temperature ballistic AC conductance of the four-channel periodic nanowire given by

$$g(\mu,\omega,0) = \frac{8\ e^2t^2}{\pi(N-1)^2\hbar^3\omega^2}\sum_{\beta=1}^{4}\left[1-\frac{(\mu-E_\beta)^2}{4t^2}\right]\left\{1-\cos\frac{(N-1)\ \hbar\omega}{2t\sqrt{1-[(\mu-E_\beta)/2t]^2}}\right\}\Xi\ (2|t|-|\mu-E_\beta|) \tag{6}$$

where $E_\beta = -2t,\ 0,\ 0,\ 2t$.

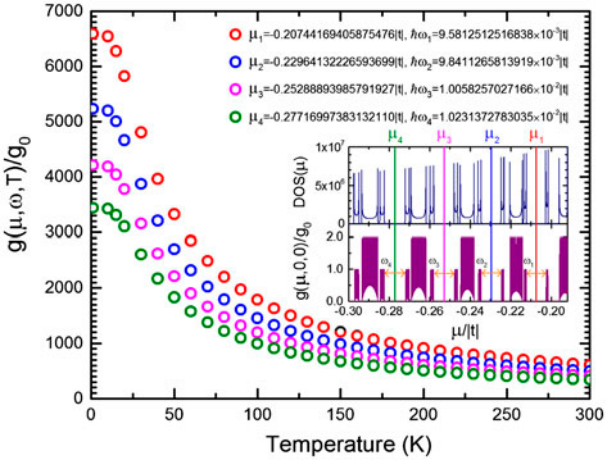

Figure 5. (colour online) AC electrical conductance $[g(\mu,\omega,T)]$ as a function of the temperature (T) for the same nanowire of Figure 4(a) and four chemical potentials (μ_j). Insets: positions of μ_j in the density of states (DOS) and zero-temperature DC conductance $[g(\mu,0,0)]$ spectra.

4. Conclusions

The impurity-induced resonant conduction analysed in this article could achieve truly large values of AC conductivity with respect to the ballistic one. In fact, these values are at least one order of magnitude larger than the results of the same phenomenon occurred in segmented nanowires [13]. This remarkable enhancement reveals the importance to explore the AC-conducting resonances in slightly perturbed ballistic systems, instead of starting from critically localized electronic states in quasiperiodically segmented nanowires.

The temperature variation analysis suggests the possibility to observe these resonant AC conducting peaks for specific electronic filling and applied electric field oscillating frequency even at room temperature. Experimentally, the chemical potential position in the band structure of a nanowire can be modified by an applied gate voltage [14].

It is also important to mention that the resonant AC conductivity observed in this work obeys the Fermi's golden rule, from which the Kubo-Greenwood formula can be deduced [15]. This rule establishes the transition probability of an electron from an eigenstate to another caused by an oscillating external field. This transition at zero temperature requires the occupation of the lower energy state and the non-occupation of the higher one; that is, the Fermi energy should be found between these two states, regardless of its specific location, as exhibited in Figures 2 and 4.

Finally, beyond the specific renormalization method used in this investigation, we would like to emphasize the possibility of performing macroscopic system studies by means of a fully real-space procedure, which allows the presence of defects, impurities and interfaces that could be very important in the design of new electronic devices.

Funding

This work has been partially supported by CONACyT-131596, UNAM-DGAPA-PAPIIT IN113813 and IN113714. Computations were performed at Miztli of DGTIC, UNAM.

References

[1] C. Janot, *Quasicrystals: A Primer*, 2nd ed., Oxford University Press, New York, 1994.
[2] C. Cheng and H.J. Fan, Nano Today 7 (2012) p.327.
[3] D.B. Suyatin, J. Sun, A. Fuhrer, D. Wallin, L.E. Fröberg, L.S. Karlsson, I. Maximov, L.R. Wallenberg, L. Samuelson and H.Q. Xu, Nano Lett. 8 (2008) p.1100.
[4] C. Kittel, *Introduction to Solid State Physics*, 8th ed., Wiley, New York, 2005.
[5] V. Sánchez and C. Wang, Phys. Rev. B 70 (2004) p.144207.
[6] A.E. Miroshnichenko, S. Flach and Y.S. Kivshar, Rev. Mod. Phys. 82 (2010) p.2257.
[7] B. Kramer and A. MacKinnon, Rep. Prog. Phys. 56 (1993) p.1469.
[8] R. Oviedo-Roa, L.A. Pérez and C. Wang, Phys. Rev. B 62 (2000) p.13805.
[9] A. Chakrabarti, Phys. Rev. B 74 (2006) p.205315.
[10] C. Wang, F. Salazar and V. Sánchez, Nano Lett. 8 (2008) p.4205.
[11] J.K. Hyun, S. Zhang and L.J. Lauhon, Annu. Rev. Mater. Res. 43 (2013) p.451.
[12] U.K. Gautam, X. Fang, Y. Bando, J. Zhan and D. Golberg, ACS Nano 2 (2008) p.1015.
[13] V. Sanchez and C. Wang, Int. J. Comput. Mater. Sci. Eng. 1 (2012) p.1250003.
[14] J. Moon, J-H. Kim, Z.C.Y. Chen, J. Xiang and R. Chen, Nano Lett. 13, 1196 (2013).
[15] E.N. Economou, *Green's Functions in Quantum Physics*, 3rd ed., Springer, Berlin, 2006.